

INHERENTLY UNSTABLE INTERNAL GRAVITY WAVES

Y. LIANG & M.-R. ALAM

Department of Mechanical Engineering, University of California, Berkeley

ABSTRACT. Here we show that there exist internal gravity waves that are inherently unstable, that is, they cannot exist in nature for a long time. The instability mechanism is a one-way (irreversible) harmonic-generation resonance that permanently transfers the energy of an internal wave to its higher harmonics. We show that, in fact, there are countably infinite number of such unstable waves. For the harmonic-generation resonance to take place, nonlinear terms in the free surface boundary condition play a pivotal role, and the instability does not obtain if a simplified boundary condition such as rigid lid or linear form is employed. Harmonic-generation resonance presented here also provides a mechanism for the transfer of the energy of the internal waves to the higher-frequency part of the spectrum where internal waves are more prone to breaking, hence losing energy to turbulence and heat and contributing to oceanic mixing.

1. INTRODUCTION

Internal gravity waves, outcome of perpetually agitated density-stratified oceans, are known to play a critical role in the dynamics of our planet's energy balance: they absorb energy to form, carry energy over long distances as they propagate, and release energy where they break (*Staquet and Sommeria*, 2002). The latter phenomenon usually gives rise to considerable mixing (c.f. *Ferrari and Wunsch*, 2008) whereby nutrients also get distributed, which is vital for a wide range of marine life (*Boyd*, 2007; *Harris*, 2012).

More than a century long research has shed a lot of light on various features of internal gravity waves. Nevertheless, many aspects of their inception and fate is yet not well understood (e.g. *Alford et al.*, 2015). Specifically, the precise mechanism that transfers energy from longer waves to high-frequency part of the spectrum, where internal waves are more prone to breaking, is yet a matter of dispute. Aside from linear processes such as interaction of internal waves with the seabed topography and sloped continental shelves (e.g. *Zhang et al.*, 2008; *Zhang and Swinney*, 2014), several nonlinear instability mechanisms have also been put forward. For instance, we now know that internal waves may undergo instability due to sideband perturbations (*Davis and Acrivos*, 1967; *Hasselmann*, 1967), or resonance triads (*Thorpe*, 1968; *McComas and Bretherton*, 1977; *Jiang and Marcus*, 2009; *Scolan et al.*, 2013; *Alam et al.*, 2009a,b, 2011; *Alam*, 2012a). All discovered destabilizing mechanisms for an internal wave (few named above), however, have one thing in common that they require some type of perturbations in order to get initiated. These perturbations can come from, for instance, seabed corrugations or presence of other waves forming resonance triads.

Here, we show that there are internal gravity waves in the ocean that are *inherently* unstable, that is, they simply cannot sustain their form. Through the mechanism studied here, specific internal waves *naturally* (without requiring any perturbation) give up their energy *permanently* to their higher harmonics through a one-way irreversible harmonic-generation resonance mechanism.

2. GOVERNING EQUATIONS AND THE DISPERSION RELATION

To see how such instability works, consider the propagation of internal waves in an inviscid, incompressible, adiabatic and stably stratified fluid of density $\rho(x, y, z, t)$, bounded by a free surface on the top and a rigid seafloor at the depth h . Let's define a Cartesian coordinate system with x, y -axes on the mean free surface and z -axis positive upward. Newton's second law, conservation of mass, and conservation of energy provide five equations for the evolution of the components of the velocity vector $\mathbf{u} = \{u, v, w\}$, density ρ , and the pressure p . These governing equations together with three boundary conditions (two kinematic boundary conditions on the free surface and the seabed, and one dynamic boundary condition on the free surface) uniquely determine the five unknowns and also solve for the surface elevation $\eta(x, y, t)$ (e.g. *Thorpe*, 1966).

E-mail address: yliang1213@berkeley.edu, reza.alam@berkeley.edu.

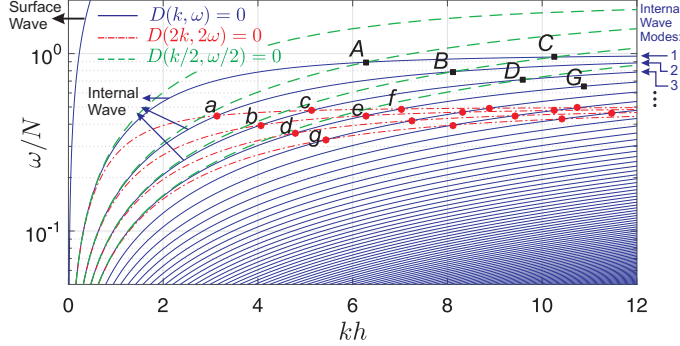


FIGURE 1. Plot of the dimensionless frequency ω/N as a function of dimensionless wavenumber kh of free internal waves (i.e. $\mathcal{D}(k, \omega) = 0$) in a fluid of linearly stratified density $\rho(z) = \rho_0(1 - az)$, with $ah = 0.05$. Associated with each wavenumber there is one surface wave and an infinite number of internal wave modes (blue solid-line branches). Frequency of internal waves cannot exceed the Brunt-Väisälä frequency N , and all branches of the dispersion relation curve are capped at $\omega/N=1$. We also plot contours of $\mathcal{D}(2k, 2\omega)=0$ (red dash-dotted lines) whose intersections with blue lines (shown by red circles) mark waves whose second harmonics are also solutions to the dispersion relation. These second harmonics are at the intersections of contours of $\mathcal{D}(k/2, \omega/2)=0$ (green dashed lines) and $\mathcal{D}(k, \omega)=0$ and are marked by black squares. The second harmonic of the wave at “a” (mode 2), is the wave “A” (mode 1) and so on. Note that second harmonic waves are at least one mode lower than the original waves.

We assume internal waves are small perturbations to a stable background state at equilibrium. Therefore, density can be written as $\rho(x, y, z, t) = \bar{\rho}(z) + \rho'(x, y, z, t)$ where $\bar{\rho}(z)$ is the background (unperturbed) density. Similarly, we define a pressure perturbation p' via $p = \bar{\rho}(z) + p'(x, y, z, t)$ such that $d\bar{\rho}(z)/dz = -\bar{\rho}(z)g$. With some standard manipulation, the governing equations can be written in terms of either of the five variables involved in this problem. We choose to write the equation, as is customary, in terms of the vertical component of the velocity, w . These equations then read (see e.g. Thorpe, 1966, or Appendix)

$$(2.1a) \quad \frac{\partial^2}{\partial t^2} \nabla^2 w + N^2 \nabla_H^2 w = \mathcal{E}(\mathbf{u}, \rho'), \quad -h < z < \eta,$$

$$(2.1b) \quad \frac{\partial^3 w}{\partial z \partial t^2} - g \nabla_H^2 w = \mathcal{F}(\mathbf{u}, p', \eta), \quad z = 0,$$

$$(2.1c) \quad w = 0, \quad z = -h.$$

where $\nabla_H^2 = \partial^2/\partial x^2 + \partial^2/\partial y^2$ is the horizontal Laplacian, $N^2 = -g/\rho_0 d\bar{\rho}(z)/dz$ is the Brunt-Väisälä frequency in which $\rho_0 = \bar{\rho}(z=0)$ is the mean density on the free surface, and \mathcal{E}, \mathcal{F} are nonlinear functions of their arguments.

To perform a perturbation analysis, we assume that the solution to (2.1) can be expressed in terms of a convergent series, i.e.

$$(2.2) \quad w(\mathbf{x}, t) = \varepsilon w^{(1)}(\mathbf{x}, t) + \varepsilon^2 w^{(2)}(\mathbf{x}, t) + \mathcal{O}(\varepsilon^3),$$

where $\varepsilon \ll 1$ is a measure of steepness of the waves involved and $w^{(i)} \sim \mathcal{O}(1)$. Similar expressions hold for u, v, ρ' and p' . Substituting (2.2) into (2.1) and collecting terms of the same magnitude, then at the leading order $\mathcal{O}(\varepsilon)$ the linearized equations obtain.

We focus our attention here on the two-dimensional problem with a linear mean density profile, i.e. $\bar{\rho}(z) = \rho_0(1 - az)$ which gives a constant Brunt-Väisälä frequency $N = \sqrt{ga}$ (c.f. e.g. Martin *et al.*, 1972). Looking for a progressive wave solution of the leading order (linearized) equation in the form $w^{(1)} = W(z) \sin(\mathbf{k} \cdot \mathbf{x} - \omega t)$ the following dispersion relations result:

$$(2.3) \quad \mathcal{D}(k, \omega) = \begin{cases} \omega^2 - \frac{gk}{\sqrt{1-N^2/\omega^2}} \tanh \left(kh \sqrt{1-N^2/\omega^2} \right) = 0, & \omega > N \\ \omega^2 - \frac{gk}{\sqrt{N^2/\omega^2-1}} \tan \left(kh \sqrt{N^2/\omega^2-1} \right) = 0, & \omega < N \end{cases}$$

Solutions to the above dispersion relation identify permissible frequency and wavenumber of free propagating waves. Contours of $\mathcal{D}(k, \omega) = 0$ are shown in figure 1 in which we plot the dimensionless frequency ω/N as a function of dimensionless wavenumber kh (blue solid curves). For $\omega > N$ only one solution exists in the first quadrant (with its mirrors in the other quadrants). This solution corresponds to a wave whose associated fluid particle motion is maximum near the free surface and decreases as the depth increases. Therefore this is basically a classical *surface* wave which is a little perturbed because of stratification. For $\omega < N$ there is an infinite number of solutions to (2.3). The first member of this set, is the continuation of the surface wave branch (the left-most branch in figure 1), but the rest identify waves with associated fluid particle activities that are minimum near the free surface and the seabed, but gain one (or more) maximum/maxima somewhere inside the fluid domain. Therefore these branches show *internal* waves. The number of maxima in the amplitude of velocity along the vertical water line determines the mode number of the branch (the first three are marked on the right-side of figure 1 with arrows). A cut-off frequency $\omega/N=1$ sets an upper frequency limit for internal waves. It is to be noted that the dispersion relation (2.2), although has a different form, is in fact graphically very close to the one under rigid lid assumption $\omega = N/\sqrt{1 + (n\pi/kh)^2}$. But clearly the inclusion of the effect of the free surface in the former has changed its form.

3. HARMONIC GENERATION

With the linear solution to (2.1) and its properties at hand, we move to the second order equation by collecting $\mathcal{O}(\epsilon^2)$ terms obtained from the substitution of (2.2) into (2.1). The second order equation has the exact same form as of the leading order equation on its left-hand side, but with nonlinear terms, arising from nonlinear functions \mathcal{E}, \mathcal{F} , on its right-hand side. These nonlinear terms are multiplication of the linear solution (and its derivatives) and, it turns out that, they constitute forcing terms with wavenumber and frequency $(2k, 2\omega)$. Now if $\mathcal{D}(2k, 2\omega)=0$, then it means that these forcing terms have a harmonic which is the same as the natural harmonic of the linear system. This is a resonance scenario through which a new second order solution may emerge and may grow large enough to the extent that it becomes comparable to the leading order solution (beyond which the naive expansion (2.2) is not valid anymore). We would like to note a subtle point here that at the second order the right-side of (2.1a) is identically zero (see e.g. *Tabaei et al.*, 2005). Therefore a potential harmonic-generation resonance is only possible through the nonlinear terms in the free surface boundary condition (2.1b). If a rigid-lid assumption or a linearized form of the free surface boundary condition is employed (which is usually the case in the investigation of internal waves) the resonance harmonic generation will simply not obtain.

To see whether it is possible to satisfy the resonance condition required for the second harmonic of an internal wave to exist as a free propagating wave, we also plot in figure 1 the contours of $\mathcal{D}(2k, 2\omega)=0$ (red dash-dotted curves) for first four internal wave modes. Intersections of these contours with the contours of $\mathcal{D}(k, \omega)=0$ (solid blue curves) identify waves whose second harmonics are also solution to the dispersion relation. Some of these intersections are marked in figure 1 by red circles and are identified by lowercase characters. It is easy to find the corresponding second harmonic by multiplying a designated (red circle) frequency and wavenumber by a factor of two, or alternatively by finding intersections of contours of $\mathcal{D}(k/2, \omega/2)=0$ (green dashed curves) and $\mathcal{D}(k, \omega)$ (denoted by black squares and uppercase characters). Specifically, “*A*” is the second harmonic of “*a*”, “*B*” is the second harmonic of “*b*” and so on. It is to be noted that the second harmonic of an internal wave always belongs to a lower mode than the mode of the original wave. For example, second harmonic of wave “*a*” (mode 2) is the wave “*A*” (mode 1), and second harmonic of wave “*c*” (mode 3) is the wave “*C*” (mode 1).

A comprehensive collection of all internal waves (for $kh < 12$) whose second harmonics are also free propagating waves is shown in figure 2. We are basically plotting in this figure all intersections points of contours of $\mathcal{D}(k, \omega) = 0$ and contours of $\mathcal{D}(2k, 2\omega) = 0$. Clearly there will be an infinite (but countable) number of such solutions. Through the approach described above, a similar exercise can be performed for waves with their third harmonic being free waves. These solutions are marked by blue circles in figure 2, and waves with their fourth harmonics lie on the dispersion relation curves are shown by green triangles, and this search can continue indefinitely.

4. THE ENERGY TRANSFER RATE

To determine the strength of the resonance (i.e. the rate of growth of the resonant wave), and the dynamics of the energy interplay between a wave and its second harmonic, here we perform a multiple scale perturbation analysis. The basic assumption is that the amplitude of the original wave and its second harmonic are both functions of spatial variables and time (i.e. \mathbf{x}, t), *as well as* a slow spatial variable in the direction of propagation $x_1 = \epsilon x$. Physically speaking, we allow the amplitude of both waves to *slowly* vary as waves propagate. Mathematically speaking this is

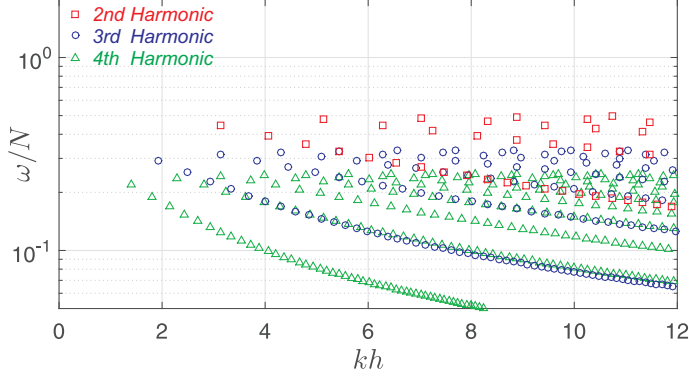


FIGURE 2. There are countably infinite number of internal waves that are unstable to their second harmonic. Physically this means that specific incident internal waves of wavenumber and frequency (k, ω) will give up their energy permanently (in a one-way irreversible process, c.f. equation (4.2)) to their second harmonic $(2k, 2\omega)$. The necessary condition for this to happen is $\mathcal{D}(k, \omega) = \mathcal{D}(2k, 2\omega) = 0$. These waves, for the parameters of figure 1, are shown here by red squares. Similar story holds for another set of waves that are unstable to their third harmonic (blue circles, necessary condition $\mathcal{D}(k, \omega) = \mathcal{D}(3k, 3\omega) = 0$), and fourth harmonic (green triangles, $\mathcal{D}(k, \omega) = \mathcal{D}(4k, 4\omega) = 0$) and so on. Instability to higher harmonics are clearly much weaker when compared with the instability to the second harmonic.

written as

$$(4.1) \quad w(x, x_1, z, t) = \varepsilon w_1(x, x_1, z, t) + \varepsilon^2 w_2(x, x_1, z, t) + \mathcal{O}(\varepsilon^3)$$

where $w_i \sim \mathcal{O}(1)$. Expressions of the same form are assumed to hold for other variables u, p', p' and η . Similar to regular perturbation methodology, described earlier in the paper to gain insight into the problem, by substituting (4.1) into the governing equation (2.1) and collecting terms of the same order in ε , at the leading order $\mathcal{O}(\varepsilon)$ the linearized equation obtains. We assume the original wave with wavenumber and frequency k, ω has the amplitude $\mathcal{A}_1(x_1)$ and the amplitude of resonant second harmonic wave with wavenumber and frequency $2k, 2\omega$ is $\mathcal{B}_2(x_1)$. At the second order, applying a compatibility condition (to avoid unbounded solutions) the following two equations governing spatial evolution of $\mathcal{A}_1(x_1)$ and $\mathcal{B}_2(x_1)$ emerge (see Appendix for details of derivation)

$$(4.2a) \quad \frac{d\mathcal{B}_2(x_1)}{dx} = \alpha \mathcal{A}_1^2(x_1),$$

$$(4.2b) \quad \frac{d\mathcal{A}_1(x_1)}{dx} = \beta \mathcal{A}_1(x_1) \mathcal{B}_2(x_1),$$

where

$$\alpha = -\frac{K_1 \omega \cos K_2 h (6K_1 + N^2/g \sin 2K_1 h)}{gk(2K_2 h + \sin 2K_2 h)},$$

$$\beta = -\frac{k[\sin K_2 h (4K_1 \cos^2 K_1 h - 3K_1) - 2K_2 \cos K_2 h \sin 2K_1 h]}{2\omega(2K_1 h + \sin 2K_1 h)}.$$

in which $K_1 = k\sqrt{N^2 - \omega^2}/\omega$ and $K_2 = k\sqrt{N^2 - 4\omega^2}/\omega$.

Spatial evolution of the normalized amplitude of the original wave $\mathcal{A}_1/\mathcal{A}_{10}$ (where $\mathcal{A}_{10} = \mathcal{A}_1(x=0)$) and its second harmonic $\mathcal{B}_2/\mathcal{A}_{10}$ as a function of spatial distance of propagation x/λ_i (where $\lambda_i = 2\pi/k$ wavelength of the original wave) is shown in figure 3 respectively by blue-dashed line and solid-red line. In accordance with the case presented in figure 1, we choose $ah=0.05$ and if we consider that waves are propagating in a water of depth $h=1$ km, then $N=0.02$ rad/s. For this case, figure 3a corresponds to the point “a” ($kh=3.144772, \omega/N=0.4472136$) with its second harmonic at “A” in figure 1, and figure 3b corresponds to point “c” ($kh=5.132426, \omega/N=0.4780914$) with its second harmonic at “C”. In the former case the interaction is (spatially) faster by a factor of about two, while in the latter case the relative amplitude of the resonant wave is higher. The most striking aspect of the solution is that the interaction is one-way. This can be seen from (4.2a) in which, because \mathcal{A}_1^2 is always positive, then $d\mathcal{B}_2/dx_1$ can never change sign. As a result the magnitude of \mathcal{B}_2 can only increase (the sign of α only contributes to 0 or π radian phase shift to the wave), and

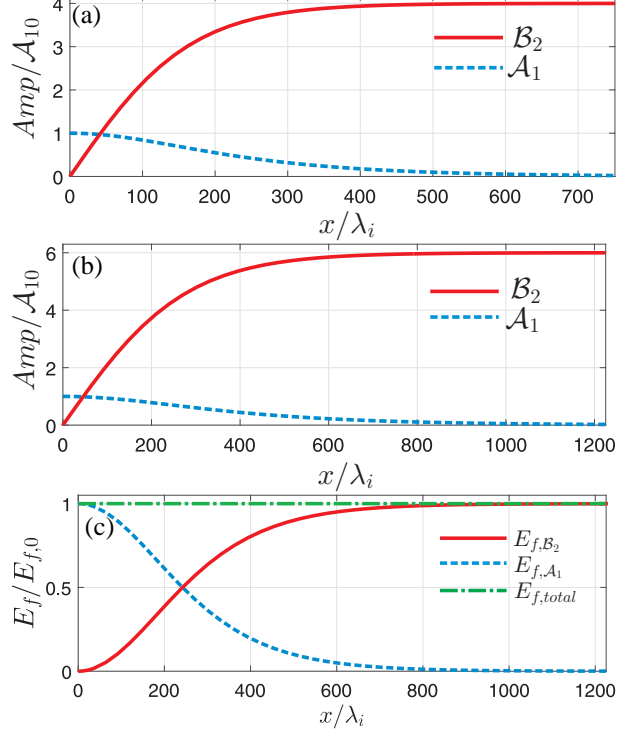


FIGURE 3. Spatial evolution of the amplitude of the original wave (blue dashed line) and its resonant second harmonic (red solid line) correspond to the point “a” in figure 1 ($kh=3.144772$, $\omega/N=0.4472136$, $aA_{10}/N=0.0023$, fig. a), and the point “c” in figure 1 ($kh=5.132426$, $\omega/N=0.4780914$, $aA_{10}/N=0.0023$, fig. b). In figure (a) energy goes from mode 2 to mode 1, whereas in figure (b) energy goes from mode 3 to mode 1. Figure (c) shows the energy flux of each wave as well as the sum of the energy fluxes (green dash-dotted line). As expected from energy conservation, the overall energy flux is unchanged in the domain of interaction.

that's why the direction of energy can never change. This is in contrast to typical triad resonance interactions (e.g. *Alam et al.*, 2010; *Alam*, 2012b) and harmonic generation in shallow water waves (e.g. *Alam and Mei*, 2007) where energy initially flows from original waves to resonant waves, but then when the amplitude of resonant waves is large enough the flow of energy reverses. Here, energy only goes from the original wave to the second harmonic and stays there permanently. The original wave will be gone forever.

Our multiple scales results conserve energy, as expected. In figure 3c (which corresponds to the case presented in figure 3b) we plot the energy flux ($E_f = E \times C_g$ where E is the energy per unit area and C_g is the group velocity) normalized by the energy flux of the original wave at the beginning ($E_{f,A_{10}}$). Plotted are the normalized energy flux of the original wave E_{f,A_1} (blue-dashed line), the second harmonic E_{f,B_2} , and the summation of the fluxes $E_{f,total} = E_{f,A_1} + E_{f,B_2}$. As expected from the conservation of energy the latter is constant and equal to unity.

To cross validate our results with direct simulation, we use the adaptive Navier-Stokes solver code SUNTANS (Stanford Unstructured Nonhydrostatic Terrain-following Adaptive Navier-Stokes Simulator (*Fringer et al.*, 2006)). As a nonhydrostatic parallel ocean model with the capability to implement nonlinear free surface, SUNTANS has been validated and widely used in studying internal waves (and associated turbulence and mixing) in stratified waters (*Zhang et al.*, 2011; *Kang and Fringer*, 2010; *Wang et al.*, 2011; *Kang and Fringer*, 2012; *Walter et al.*, 2012; *Zhang et al.*, 2011; *Wang et al.*, 2011).

Here we consider propagation of waves in a stratified water of density gradient $a = 1 \times 10^{-3} \text{ m}^{-1}$, depth 100m and in a domain of horizontal extent 20km. We choose 5×10^3 grid points in the x direction and 100 layers in the z direction. We specify the velocity of fluid particle at the left boundary to match that of desired incoming wave. Therefore the left boundary that serves as the incoming wave boundary (wave maker). We set the right-side vertical boundary of the domain as the no-penetration and slip-free, and therefore it will act as a rigid vertical wall. We consider the case of incident internal wave of mode 2 ($kh=3.147946$, $\omega/N=0.4472136$, vertical velocity amplitude $w=0.1\text{m/s}$) with its

second harmonic being a mode 1 wave. The time step $\delta t/T=1/35000$ where T is the period of the incident wave. We run the simulation until the incident wave arrives at the wall, at which point amplitude of both waves (incident and its second harmonics) have reached a steady state in the domain of interest $0 < x/\lambda_i < 20$. The curve of $\mathcal{B}_2/\mathcal{A}_{10}$ vs x/λ_1 gives an initial slope of 0.0107 which is the same as our theoretical prediction (4.2).

5. CONCLUSION

Here we reported that certain internal gravity waves are inherently unstable and are not able to sustain their form. This new instability mechanism, a result of resonance harmonic-generation, draws the energy of an internal wave and hands it over to its second (or generally higher) harmonic. This resonance is distinguished from the classical triad resonance (and associated subharmonic instability) in that 1- a single wave may undergo the instability without requiring any external perturbation, and 2- the transfer of energy is irreversible and the original wave permanently loses its energy to its second harmonic. Extension of the results presented here to the third and higher harmonic generation is straightforward, but the strength of energy exchange in higher harmonics is much weaker. It can be shown that a qualitatively-similar harmonic generation resonance occurs in a wide range of depth-dependent density profiles $N = N(z)$ (e.g. parabolic, exponential, etc). Harmonic-generation resonance presented here, and its associated near-resonance, also provides a mechanism for the transfer of the energy of a wide range of internal waves to the higher-frequency part of the spectrum where internal waves are more prone to breaking, hence losing energy to turbulence and heat and contributing to oceanic mixing.

APPENDIX: DERIVATION OF THE INTERACTION EQUATION

Consider the propagation of waves in an inviscid, incompressible, adiabatic and stably stratified fluid of density $\rho(x, y, z, t)$, bounded by a free surface on the top and a rigid seafloor with a depth h at the bottom. We consider a Cartesian coordinate system with x, y -axes on the mean free surface and z -axis positive upward. Equations governing the evolution of the velocity vector $\mathbf{u} = \{u, v, w\}$, density ρ , pressure p and surface elevation η under Boussinesq approximation read

$$\begin{aligned}
 (5.1a) \quad & \rho_0 \frac{D\mathbf{u}}{Dt} = -\nabla p - \rho g \nabla z, \quad -h + b < z < \eta \\
 (5.1b) \quad & \frac{D\rho}{Dt} = 0, \quad -h + b < z < \eta \\
 (5.1c) \quad & \nabla \cdot \mathbf{u} = 0, \quad -h + b < z < \eta \\
 (5.1d) \quad & \eta_t = \mathbf{u} \cdot \nabla(z - \eta), \quad z = \eta \\
 (5.1e) \quad & \frac{Dp}{Dt} = 0, \quad z = \eta \\
 (5.1f) \quad & w = 0, \quad z = -h,
 \end{aligned}$$

where g is the gravitational acceleration, and $\rho_0 = \bar{\rho}(z=0)$ is the mean density on the free surface with $\bar{\rho}(z)$ the background (unperturbed) density such that $\rho = \bar{\rho}(z) + \rho'(x, y, z, t)$. Equation (5.1a) is the momentum equating (Euler's equations), (5.1b) comes from conservation of energy, and (5.1c) is continuity equation that together form five equations for five unknown variables of the problem (the components of velocity \mathbf{u} , pressure p and density ρ). Equations (5.1d)-(5.1f) are boundary conditions on the free surface and the bottom.

Similar to the density perturbation ρ' , we define a pressure perturbation p' via $p = \bar{p}(z) + p'(x, y, z, t)$ such that $d\bar{p}(z)/dz = -\bar{\rho}(z)g$. For the linear terms of the governing equation (5.1a) to be only in terms of w we calculate $\partial/\partial z[\nabla \cdot (5.1a)] - \nabla^2(5.1a)_3$, where $(5.1a)_3$ denotes the z component of (5.1a) (likewise, 1,2 for x, y will be used later). We obtain

$$(5.2) \quad \frac{\partial}{\partial t} \nabla^2 w - \frac{\partial^2}{\partial x \partial z} \mathbf{u} \cdot \nabla u - \frac{\partial^2}{\partial y \partial z} \mathbf{u} \cdot \nabla v + \nabla_H^2(\mathbf{u} \cdot \nabla w) + \frac{g}{\rho_0} \nabla_H^2 \rho' = 0.$$

where $\nabla_H^2 = \partial^2/\partial x^2 + \partial^2/\partial y^2$ is the horizontal Laplacian. Taking the time derivative of (5.2) and substituting ρ' from the expansion of (5.1b), i.e.,

$$(5.3) \quad \frac{\partial \rho'}{\partial t} + \mathbf{u} \cdot \nabla \rho' + w \frac{d\bar{p}(z)}{dz} = 0.$$

and denoting $N^2 = -g/\rho_0 d\bar{\rho}/dz$ as the Brunt-Väisälä frequency, we obtain

$$(5.4) \quad \frac{\partial^2}{\partial t^2} \nabla^2 w + N^2 \nabla_H^2 w = \frac{\partial^3}{\partial x \partial z \partial t} \mathbf{u} \cdot \nabla u + \frac{\partial^3}{\partial y \partial z \partial t} \mathbf{u} \cdot \nabla v - \nabla_H^2 \frac{\partial}{\partial t} (\mathbf{u} \cdot \nabla w) + \frac{g}{\rho_0} \nabla_H^2 (\mathbf{u} \cdot \nabla \rho').$$

To perform a weakly nonlinear analysis, we assume that internal waves in the system described above are small perturbations from the mean state of water at rest, i.e. $\mathbf{u}, \rho', \mathbf{p}' \sim \mathcal{O}(\varepsilon)$, where ε is a measure of the wave steepness. Expanding the surface dynamic boundary condition (5.1e) and keeping terms up to the second order we obtain

$$(5.5) \quad \frac{\partial p'}{\partial t} = w \rho_0 g - \mathbf{u} \cdot \nabla p' - \frac{\partial^2 p'}{\partial z \partial t} \eta + \rho_0 g \eta \frac{\partial w}{\partial z} + g \eta w \frac{d\bar{\rho}}{dz}, \text{ at } z = 0.$$

where the last term can be equivalently written as $N^2 \bar{\rho}_0 \eta w$. Here p' can be substituted from an expression obtained from taking the x derivative of (5.1a)₁ added to the y derivative of (5.1a)₂:

$$(5.6) \quad -\frac{\partial^3 w}{\partial z \partial t^2} + \frac{1}{\rho_0} \nabla_H^2 \frac{\partial p'}{\partial t} + \frac{\partial^2}{\partial x \partial t} \mathbf{u} \cdot \nabla u + \frac{\partial^2}{\partial y \partial t} \mathbf{u} \cdot \nabla v = 0.$$

Substituting $\partial p'/\partial t$ from (5.6) in (5.5) we obtain

$$(5.7) \quad \frac{\partial^3 w}{\partial z \partial t^2} - g \nabla_H^2 w = \frac{\partial^2}{\partial x \partial t} \mathbf{u} \cdot \nabla u + \frac{\partial^2}{\partial y \partial t} \mathbf{u} \cdot \nabla v + \nabla_H^2 \left(g \frac{dw}{dz} \eta + N^2 w \eta \right) - \frac{1}{\rho_0} \nabla_H^2 \left(\mathbf{u} \cdot \nabla p' + \frac{\partial^2 p'}{\partial z \partial t} \eta \right).$$

Therefore the governing equation and boundary conditions correct to $\mathcal{O}(\varepsilon^2)$ reduce to (5.4), (5.7) and (5.1f). For the ease of referring, we rewrite these equations here:

(5.8a)

$$\frac{\partial^2}{\partial t^2} \nabla^2 w + N^2 \nabla_H^2 w = \frac{\partial^3}{\partial x \partial z \partial t} \mathbf{u} \cdot \nabla u + \frac{\partial^3}{\partial y \partial z \partial t} \mathbf{u} \cdot \nabla v - \frac{\partial^3}{\partial x^2 \partial t} \mathbf{u} \cdot \nabla w - \frac{\partial^3}{\partial y^2 \partial t} \mathbf{u} \cdot \nabla w + \frac{g}{\rho_0} \nabla_H^2 (\mathbf{u} \cdot \nabla \rho') - h < z < 0,$$

(5.8b)

$$\frac{\partial^3 w}{\partial z \partial t^2} - g \nabla_H^2 w = \frac{\partial^2}{\partial x \partial t} \mathbf{u} \cdot \nabla u + \frac{\partial^2}{\partial y \partial t} \mathbf{u} \cdot \nabla v + \nabla_H^2 \left(g \frac{dw}{dz} \eta + N^2 w \eta \right) - \frac{1}{\rho_0} \nabla_H^2 \left(\mathbf{u} \cdot \nabla p' + \frac{\partial^2 p'}{\partial z \partial t} \eta \right) z = 0,$$

(5.8c)

$$w = 0, z = -h.$$

Equations (5.8a) and (5.8b) are identical to equations (A2) and (A7) of Thorpe 1966¹ (*Thorpe (1966)*).

Considering the two-dimensional problem and assuming that the solution to this problem can be expressed in terms of a convergent series we define

$$(5.9) \quad w(x, x_1, z, t) = \varepsilon w_1(x, x_1, z, t) + \varepsilon^2 w_2(x, x_1, z, t) + \mathcal{O}(\varepsilon^3)$$

where $x_1 = \varepsilon x$ is the slow spatial variable with $\varepsilon \ll 1$ is a measure of steepness of the waves and $w_i \sim \mathcal{O}(1)$. Similar expressions exist for other variables, i.e. $u = \varepsilon u_1 + \varepsilon^2 u_2 + \mathcal{O}(\varepsilon^3)$, $\rho' = \varepsilon \rho'_1 + \varepsilon^2 \rho'_2 + \mathcal{O}(\varepsilon^3)$, $p' = \varepsilon p'_1 + \varepsilon^2 p'_2 + \mathcal{O}(\varepsilon^3)$ and $\eta = \varepsilon \eta_1 + \varepsilon^2 \eta_2 + \mathcal{O}(\varepsilon^3)$ with $u_i, \rho'_i, p'_i \sim \mathcal{O}(1)$ being functions of x, x_1, z, t , and $\eta_i \sim \mathcal{O}(1)$ being functions of x, x_1 and t .

Upon substitution into the governing equation, at the leading order $\mathcal{O}(\varepsilon)$ we obtain

$$(5.10a) \quad \frac{\partial^2}{\partial t^2} \nabla^2 w_1 + N^2 \nabla_H^2 w_1 = 0 \quad -h < z < 0,$$

$$(5.10b) \quad \frac{\partial^3 w_1}{\partial z \partial t^2} - g \nabla_H^2 w_1 = 0 \quad z = 0,$$

$$(5.10c) \quad w_1 = 0, \quad z = -h.$$

At the second order $\mathcal{O}(\varepsilon^2)$ we have

$$\frac{\partial^2}{\partial t^2} \nabla^2 w_2 + N^2 \nabla_H^2 w_2 = -2 \left(\frac{\partial^2}{\partial t^2} + N^2 \right) \frac{\partial^2}{\partial x \partial x_1} w_1 + \frac{\partial^3}{\partial x \partial z \partial t} \mathbf{u}_1 \cdot \nabla u_1 + \frac{\partial^3}{\partial y \partial z \partial t} \mathbf{u}_1 \cdot \nabla v_1 - \frac{\partial^3}{\partial x^2 \partial t} \mathbf{u}_1 \cdot \nabla w_1$$

¹except that we found three typos there: (1) for $S1$ in (A2), the sign of the last term with g should be positive; (2) for $S3$ in (A7), the first term should be $\mathbf{u} \cdot \nabla w$; and (3) the term $g \nabla_1^2 \frac{\partial}{\partial x} (\eta w_z)$ is missing. These are clearly typos as they do not appear in later expressions of *Thorpe (1966)*.

$$(5.11a) \quad -\frac{\partial^3}{\partial y^2 \partial t} \mathbf{u}_1 \cdot \nabla w_1 + \frac{g}{\rho_0} \nabla_H^2 (\mathbf{u}_1 \cdot \nabla p'_1), \quad -h \leq z \leq 0.$$

$$(5.11b) \quad \frac{\partial^3 w_2}{\partial z \partial t^2} - g \nabla_H^2 w_2 = 2g \frac{\partial^2 w_1}{\partial x \partial t} + \frac{\partial^2}{\partial x \partial t} \mathbf{u}_1 \cdot \nabla u_1 + \frac{\partial^2}{\partial y \partial t} \mathbf{u}_1 \cdot \nabla v_1 + \nabla_H^2 \left(g \frac{dw_1}{dz} \eta_1 + N^2 w_1 \eta_1 \right) - \frac{1}{\rho_0} \nabla_H^2 \left(\mathbf{u}_1 \cdot \nabla p'_1 + \frac{\partial^2 p'_1}{\partial z \partial t} \eta_1 \right), \quad z = 0.$$

$$(5.11c) \quad w_2 = 0, \quad z = -h.$$

We now assume that waves with wavenumber and frequency (k, ω) and $(2k, 2\omega)$ satisfy the internal waves dispersion relation (which obtains from the linear equation (5.10))

$$(5.12) \quad \mathcal{D}(k, \omega) = \omega^2 - \frac{gk}{\sqrt{ga/\omega^2 - 1}} \tan \left(kh \sqrt{ga/\omega^2 - 1} \right),$$

i.e. $\mathcal{D}(k, \omega) = 0$ and $\mathcal{D}(2k, 2\omega) = 0$, and that they both exist in our domain of interest, though potentially with different amplitudes. Propagating wave solution to the linear equation (5.10) then obtains as

$$(5.13a) \quad w_1(x, x_1, z, t) = A_1(x_1) \sin K_1(z + h) \sin(kx - \omega t) + B_1(x_1) \sin K_1(z + h) \cos(kx - \omega t)$$

$$(5.13b) \quad + A_2(x_1) \sin K_2(z + h) \sin(2kx - 2\omega t) + B_2(x_1) \sin K_2(z + h) \cos(2kx - 2\omega t)$$

in which A_1, A_2, B_1, B_2 are amplitudes of each wave, $K_1^2 = k^2(N^2 - \omega^2)/\omega^2$ and $K_2^2 = k^2(N^2 - 4\omega^2)/\omega^2$. Other variables u, p', p' and η can be found respectively via continuity equation (5.1c), energy equation (5.1b), kinematic surface boundary condition (5.1d) and the dynamic free surface boundary condition (5.1f).

The left-hand side of the second order equation (5.11) is identical in the form to the first order equation (5.10), but the right hand side of (5.11) is clearly non-zero and is a nonlinear function of leading order solution $\mathbf{u}_1, \rho'_1, p'_1, \eta_1$. It turns out, after substitution, that the right hand side contains terms with harmonics which are the same as the harmonics of the leading order equation (secular terms). A compatibility condition then must be enforced to make sure that the solution does not go unbounded, which is clearly unphysical. This compatibility condition determines the spatial behavior of the coefficients A_i, B_i .

While the formulation presented here is general, our primary interest is when an initial wave with wavenumber and frequency (k, ω) *resonates* its second harmonic $(2k, 2\omega)$ whose initial amplitude is zero. Therefore in the following we use the adjectives *original* and *resonant* waves to refer to (k, ω) and $(2k, 2\omega)$ waves respectively. We would like to emphasize that the formulation is general and works for any initial condition of the two waves. We will also comment that the presented approach can be easily extended for third and higher-harmonic generation.

Without loss of generality we assume that $B_1 = 0$, which only has to do with our choice of coordinate system. But we keep A_2 and B_2 , since they determine the phase of the resonant wave $(2k, 2\omega)$ with respect to the original wave (k, ω) . The general solution to the second order problem takes the form

$$(5.14a) \quad w_2(x, x_1, z, t) = C_{11}(x_1, z) \sin(kx - \omega t) + C_{12}(x_1, z) \cos(kx - \omega t)$$

$$(5.14b) \quad + C_{21}(x_1, z) \sin(2kx - 2\omega t) + C_{22}(x_1, z) \cos(2kx - 2\omega t)$$

where $C_{ij}(x_1, z)$'s are to be determined from (5.11). Substituting (5.14) and (5.13) into (5.11), and collecting same sine and cosine terms we obtain four ordinary differential equations for C_{ij} ($i, j=1,2$):

$$(5.15a) \quad -\omega^2 C_{1i,zz} - K_1^2 \omega^2 C_{1i} = E_{1i}, \quad -h < z < 0,$$

$$(5.15b) \quad -\omega^2 C_{1i,z} + gk^2 C_{1i} = F_{1i}, \quad z = 0,$$

$$(5.15c) \quad C_{1i} = 0, \quad z = -h,$$

$$(5.16a) \quad -4\omega^2 C_{2i,zz} - 4K_2^2 \omega^2 C_{2i} = E_{2i}, \quad -h < z < 0,$$

$$(5.16b) \quad -4\omega^2 C_{2i,z} + 4gk^2 C_{2i} = F_{2i}, \quad z = 0,$$

$$(5.16c) \quad C_{2i} = 0, \quad z = -h,$$

where E_{1i}, F_{1i} are the coefficients of $\sin(ikx - i\omega t)$, and E_{i2}, F_{i2} are the coefficients of $\cos(ikx - i\omega t)$ in the right-hand side of (5.11a) and (5.11b) respectively. Let's first consider the equation for C_{22} , we obtain

$$(5.17) \quad E_{22} = -\frac{4\omega^2 K_2^2}{k} \sin K_2(z + h) \frac{dA_2(x_1)}{dx_1}, \quad F_{22} = 4gk \sin K_2 h \frac{dA_2(x_1)}{dx_1}$$

for which the solution to (5.16a) that satisfies the boundary condition (5.16c) is

$$(5.18) \quad C_{22}(x_1, z) = -\frac{K_2}{2k}(z+h) \cos K_2(z+h) \frac{dA_2(x_1)}{dx_1}.$$

Upon substitution into (5.16b) we obtain

$$(5.19) \quad gk \left(\frac{2K_2h + \sin 2K_2h}{\cos K_2h} \right) \frac{dA_2(x_1)}{dx_1} = 0$$

therefore, since the coefficient is nonzero then $dA_2/dx_1 \equiv 0$. Physically speaking, this expression says that the amplitude A_2 does not change as waves propagate, or in other words, A_2 does not take part in the energy exchange. We, therefore, set A_2 equal to zero for the rest of the derivation.

We use the same approach as above for C_{21} . We have

$$(5.20) \quad E_{21} = \frac{4\omega^2 K_2^2}{k} \sin K_2(z+h) \frac{dB_2(x_1)}{dx_1}, \quad F_{21} = -4gk \sin K_2h \frac{dB_2}{dx_1} - 2 \left(3\omega K^2 + \frac{N^2 k^2}{\omega} \sin^2 K_1 h \right) A_1^2(x_1)$$

for which

$$(5.21) \quad C_{21}(x_1, z) = \frac{K_2}{2k}(z+h) \cos K_2(z+h) \frac{dB_2(x_1)}{dx_1},$$

and upon substitution into (5.16b) we obtain

$$(5.22) \quad \frac{dB_2(x_1)}{dx_1} = \alpha A_1^2(x_1),$$

where

$$(5.23) \quad \alpha = -\frac{K_1 \omega \cos K_2 h (6K_1 + N^2/g \sin 2K_1 h)}{gk(2K_2h + \sin 2K_2h)}.$$

For $C_{11}(x_1, z)$, we obtain $E_{11} = F_{11} = 0$ and therefore the equation for $C_{11}(x_1, z)$ does not provide any extra information on $A_1(x_1)$ and $B_2(x_1)$. For C_{12} we obtain

$$(5.24) \quad E_{21} = \frac{2K^2 \omega^2}{k} \sin K_1(z+h) \frac{dA_1(x_1)}{dx_1} + \{ I^+ \sin [(K_1 + K_2)(z+h)] + I^- \sin [(K_1 - K_2)(z+h)] \} A_1(x_1) B_2(x_1)$$

$$(5.25) \quad F_{21} = 2gk \sin K_1(z+h) \frac{dA_1(x_1)}{dx_1} + J A_1(x_1) B_2(x_1)$$

where

$$(5.26a) \quad I^+ = \frac{1}{8} \omega (K_2 + 2K_1)(K_2^2 + 3k^2 - K_1^2)$$

$$(5.26b) \quad I^- = \frac{1}{8} \omega (2K_1 - K_2)(K_1^2 - 3k^2 - K_2^2)$$

$$(5.26c) \quad J = \frac{1}{4} \frac{gk^2 (4K_1 \cos^2 K_1 h \sin K_2 h - 2K_2 \cos K_2 h \sin 2K_1 h - 3K_1 \sin K_2 h)}{\omega \cos K_1 h}.$$

We obtain

$$(5.27) \quad C_{12}(x_1, z) = -\frac{K_1}{k}(z+h) \cos K_1(z+h) \frac{dA_1(x_1)}{dx_1} + \left\{ \frac{I^+ \sin [(K_1 + K_2)(z+h)]}{\omega^2 [K_1^2 - (K_1 + K_2)^2]} + \frac{I^- \sin [(K_1 - K_2)(z+h)]}{\omega^2 [K_1^2 - (K_1 - K_2)^2]} \right\} A_1(x_1) B_2(x_1).$$

Substituting into (5.16b), we obtain

$$(5.28) \quad \frac{dA_1(x_1)}{dx_1} = \beta A_1(x_1) B_2(x_1),$$

where

$$(5.29) \quad \beta = -\frac{k[\sin K_2 h (4K_1 \cos^2 K_1 h - 3K_1) - 2K_2 \cos K_2 h \sin 2K_1 h]}{2\omega(2K_1 h + \sin 2K_1 h)}.$$

If we define the actual amplitudes $\mathcal{A}_1 = \varepsilon A_1$ and $\mathcal{B}_2 = \varepsilon B_2$ (note that $w = \varepsilon w_1 + \mathcal{O}(\varepsilon^2)$) then

$$(5.30a) \quad \frac{d\mathcal{B}_2}{dx} = \alpha \mathcal{A}_1^2$$

$$(5.30b) \quad \frac{d\mathcal{A}_1}{dx} = \beta \mathcal{A}_1 \mathcal{B}_2,$$

with the same α, β repeated here:

$$\alpha = -\frac{K_1 \omega \cos K_2 h (6K_1 + N^2/g \sin 2K_1 h)}{gk(2K_2 h + \sin 2K_2 h)},$$

$$\beta = -\frac{k[\sin K_2 h (4K_1 \cos^2 K_1 h - 3K_1) - 2K_2 \cos K_2 h \sin 2K_1 h]}{2\omega(2K_1 h + \sin 2K_1 h)}.$$

REFERENCES

Alam, M.-R. (2012a), Broadband cloaking in stratified seas, *Physical review letters*, 108(8), 084,502.

Alam, M.-R. (2012b), A new triad resonance between co-propagating surface and interfacial waves, *Journal of Fluid Mechanics*, 691, 267–278.

Alam, M.-R., and C. C. Mei (2007), Attenuation of long interfacial waves over a randomly rough seabed, *Journal of Fluid Mechanics*, 587, 73–96.

Alam, M.-R., Y. Liu, and D. K. P. Yue (2009a), Bragg resonance of waves in a two-layer fluid propagating over bottom ripples. Part II. Numerical simulation, *J. Fluid Mech.*, 624, 225–253, doi:10.1017/S002211200800548X.

Alam, M.-R., Y. Liu, and D. K. Yue (2009b), Bragg resonance of waves in a two-layer fluid propagating over bottom ripples. part ii. numerical simulation, *Journal of Fluid Mechanics*, 624, 225–253.

Alam, M.-R., Y. Liu, and D. K. Yue (2010), Oblique sub-and super-harmonic bragg resonance of surface waves by bottom ripples, *Journal of Fluid Mechanics*, 643, 437–447.

Alam, M.-R., Y. Liu, and D. K. Yue (2011), Resonant-wave signature of an oscillating and translating disturbance in a two-layer density stratified fluid, *Journal of Fluid Mechanics*, 675, 477–494.

Alford, M. H., T. Peacock, J. A. MacKinnon, J. D. Nash, M. C. Buijsman, L. R. Centuroni, S.-Y. Chao, M.-H. Chang, D. M. Farmer, O. B. Fringer, et al. (2015), The formation and fate of internal waves in the south china sea, *Nature*, 521(7550), 65–69.

Boyd, P. W. (2007), Biogeochemistry: iron findings, *Nature Reports Climate Change*, pp. 10–11.

Davis, R. E., and A. Acrivos (1967), The stability of oscillatory internal waves, *Journal of Fluid Mechanics*, 30(04), 723–736.

Ferrari, R., and C. Wunsch (2008), Ocean circulation kinetic energy: Reservoirs, sources, and sinks, *Annual Review of Fluid Mechanics*, 41(1), 253.

Fringer, O. B., M. Gerritsen, and R. L. Street (2006), An unstructured-grid, finite-volume, nonhydrostatic, parallel coastal ocean simulator, *Ocean Modelling*, 14(3-4), 139–173, doi:10.1016/j.ocemod.2006.03.006.

Harris, G. (2012), *Phytoplankton ecology: structure, function and fluctuation*, Springer Science & Business Media.

Hasselmann, K. (1967), A criterion for nonlinear wave stability, *Journal of Fluid Mechanics*, 30(04), 737–739.

Jiang, C.-H., and P. S. Marcus (2009), Selection rules for the nonlinear interaction of internal gravity waves., *Physical review letters*, 102(12), 1–4, doi:10.1103/PhysRevLett.102.124502.

Kang, D., and O. Fringer (2010), On the Calculation of Available Potential Energy in Internal Wave Fields, *Journal of Physical Oceanography*, 40(11), 2539–2545, doi:10.1175/2010JPO4497.1.

Kang, D., and O. Fringer (2012), Energetics of Barotropic and Baroclinic Tides in the Monterey Bay Area, *Journal of Physical Oceanography*, 42(2), 272–290, doi:10.1175/JPO-D-11-039.1.

Martin, S., W. Simmons, and C. Wunsch (1972), The excitation of resonant triads by single internal waves, *J. Fluid Mech.*, 53, 17–44, doi:10.1017/S0022112072000023.

McComas, C. H., and F. P. Bretherton (1977), Resonant interaction of oceanic internal waves, *Journal of Geophysical Research*, 82(9), 1397–1412.

Scolan, H., E. Ermanyuk, and T. Dauxois (2013), Nonlinear fate of internal wave attractors, *Physical review letters*, 110(23), 234,501.

Staquet, C., and J. Sommeria (2002), Internal gravity waves : from instabilities to turbulence, *Annu. Rev. Fluid Mech.*, 34, 559–593, doi:10.1146/annurev.fluid.34.090601.130953.

Tabaei, A., T. R. Akylas, and K. G. Lamb (2005), Nonlinear effects in reflecting and colliding internal wave beams, *Journal of Fluid Mechanics*, 526, 217–243, doi:10.1017/S0022112004002769.

Thorpe, S. A. (1966), On wave interactions in a stratified fluid, *J. Fluid Mech.*, 24, 737–751.

Thorpe, S. a. (1968), On the Shape of Progressive Internal Waves, *Philosophical Transactions of the Royal Society A: Mathematical, Physical and Engineering Sciences*, 263(1145), 563–614, doi:10.1098/rsta.1968.0033.

Walter, R. K., C. B. Woodson, R. S. Arthur, O. B. Fringer, and S. G. Monismith (2012), Nearshore internal bores and turbulent mixing in southern Monterey Bay, *Journal of Geophysical Research*, 117(C07017), 1–13, doi:10.1029/2012JC008115.

Wang, B., S. N. Giddings, O. B. Fringer, E. S. Gross, D. A. Fong, and S. G. Monismith (2011), Modeling and understanding turbulent mixing in a macrotidal salt wedge estuary, *Journal of Geophysical Research*, 116(C02036), 1–23, doi:10.1029/2010JC006135.

Zhang, H., B. King, and H. L. Swinney (2008), Resonant generation of internal waves on a model continental slope, *Physical review letters*, 100(24), 244,504.

Zhang, L., and H. L. Swinney (2014), Virtual seafloor reduces internal wave generation by tidal flow, *Physical Review Letters*, 112(10), 1–5, doi:10.1103/PhysRevLett.112.104502.

Zhang, Z., O. B. Fringer, and S. R. Ramp (2011), Three-dimensional, nonhydrostatic numerical simulation of nonlinear internal wave generation and propagation in the South China Sea, *Journal of Geophysical Research*, 116(C05022), 1–26, doi:10.1029/2010JC006424.